

Adversarial Examples that Fool Detectors

Jiajun Lu*, Hussein Sibai*, Evan Fabry
University of Illinois at Urbana Champaign
{jlu23, sibai2, efabry2}@illinois.edu

Abstract

An adversarial example is an example that has been adjusted to produce a wrong label when presented to a system at test time. To date, adversarial example constructions have been demonstrated for classifiers, but not for detectors. If adversarial examples that could fool a detector exist, they could be used to (for example) maliciously create security hazards on roads populated with smart vehicles. In this paper, we demonstrate a construction that successfully fools two standard detectors, Faster RCNN and YOLO. The existence of such examples is surprising, as attacking a classifier is very different from attacking a detector, and that the structure of detectors – which must search for their own bounding box, and which cannot estimate that box very accurately – makes it quite likely that adversarial patterns are strongly disrupted. We show that our construction produces adversarial examples that generalize well across sequences digitally, even though large perturbations are needed. We also show that our construction yields physical objects that are adversarial.

1. Introduction

An *adversarial example* is an example that has been adjusted to produce a wrong label when presented to a system at test time. In the literature, adversarial examples with imperceptible perturbations and unexpected properties (e.g. transferability) are one of the biggest mysteries of neural networks. There is a range of constructions [19, 21, 20] that yield adversarial examples for image classifiers, and there is good evidence that small imperceptible adjustments suffice. Furthermore, Athalye *et al.* [1] show that it is possible to build a physical object with visible perturbation patterns that is persistently misclassified by standard image classifiers from different view angles at a roughly fixed distance. There is good evidence that adversarial examples built for one classifier will fool others, too [22, 14]. The success of these attacks can be seen as a warning not to use highly non-

linear feature constructions without having strong mathematical constraints on what these constructions do; but taking that position means one cannot use methods that are largely accurate and effective.

Detectors are not classifiers. A classifier accepts an image and produces a label. In contrast, a detector, like Faster RCNN [24, 5], identifies bounding boxes that are “worth labelling”, and then generates labels (which might include background) for each box. The final label generation step employs a classifier. However, the statistics of how bounding boxes cover objects in a detector are complex and not well understood. Some modern detectors like YOLO 9000 [23] predict boxes and labels using features on a fixed grid, resulting in fairly complex sampling patterns in the space of boxes, and this means that pixels outside a box may participate in labelling that box. Another important difference is that detectors usually have ROI pooling or feature map resizing, which might be effective at disrupting adversarial patterns. To date, no successful adversarial attack on a detector has been demonstrated. In this paper, we demonstrate successful adversarial attacks on Faster RCNN, which generalize to YOLO 9000.

We also discuss the generalization ability of adversarial examples. We say that an adversarial perturbation generalizes if, when circumstances (digital or physical) change, the corresponding images remain adversarial. For example, a perturbation of a stop sign generalizes over different distances if it remains adversarial when the camera approaches the stop sign. An example generalizes better if it remains adversarial for more cases (e.g. changes of detector, background and lighting). If an adversarial example cannot generalize, it is not a threat in the majority of real world systems.

Our contributions in this paper are as follows:

- We demonstrate a method to construct adversarial examples that fool Faster RCNN digitally; examples produced by our method are reliably either missed or mislabeled by the detector. These examples without modification also fool YOLO 9000, indicating that the construction produces examples that can transfer across models.

*Both authors contributed equally

- Our adversarial examples can be physically created successfully, and they still can fool detectors in suitable circumstances. They can also slip through recent strong image processing defenses against adversarial examples.
- In practice, we find that adversarial examples require quite large disruptions to the pattern on the object in order to fool detectors. Physical adversarial examples require bigger disruptions than digital examples to succeed.

2. Background

Adversarial examples are of interest mainly because the adjustments required seem to be very small and are easy to obtain [30, 9, 8]. Numerous search procedures generate adversarial examples [19, 21, 20]; all searches look for an example that is (a) “near” a correctly labelled example (typically in L_1 or L_2 norm), and (b) mislabelled. Printing adversarial images then photographing them can retain their adversarial property [13, 1], which suggests that adversarial examples might exist in the physical world. Their existence could cause a great deal of mischief. There is some evidence that it is difficult to build physical examples that fool a stop sign detector [16]. In particular, if one actually takes a video of an existing adversarial stop sign, the adversarial pattern does not appear to affect the performance of the detector by much. Lu *et al.* speculated that this might be because adversarial patterns were disrupted by being viewed at different scales, rotations, and orientations. This created some discussion. OpenAI demonstrated a search procedure that could produce an image of a cat that was misclassified when viewed at multiple scales [1]. There is some blurring of the fur texture on the cat they generate, but this would likely be imperceptible to most observers. OpenAI also demonstrated an adversarial image of a cat that was misclassified when viewed at multiple scales *and* orientations [1]. However, there are significant visible artifacts on that image; few would think that it had not been obviously tampered with.

Recent work has demonstrated physical objects that are persistently misclassified from different angles at a roughly fixed distance [1]. The search procedure manipulates the texture map \mathcal{T} of the object. The procedure samples a set of viewing conditions \mathcal{V}_i for the object, then renders to obtain images $I(\mathcal{V}_i, \mathcal{T})$. Finally, the procedure adjusts the texture map to obtain images that are (a) close to the original images and (b) have high probability of misclassification. The adversarial properties of the resulting objects are robust to the inevitable errors in color, etc., in producing physical objects from digital representations.

Defences: There is fair evidence that it is hard to tell whether an example is adversarial (and so (a) evi-

dence of an attack and (b) likely to be misclassified) or not [27, 10, 28, 18, 4, 7]. Current procedures to build adversarial examples for deep networks appear to subvert the feature construction implemented by the network to produce odd patterns of activation in late stage ReLU’s; this can be exploited to build one form of defence [15]. There is some evidence that other feature constructions admit adversarial attacks, too [18]. However, adversarial attacks typically introduce unnatural (if small) patterns into images, and image processing methods that remove such patterns yield successful defenses. Guo *et al.* showed that cropping and rescaling, bit depth reduction, JPEG compression and decompression, resampling and reconstructing using total variation criteria, and image quilting all provide quite effective ways of removing adversarial patterns [11].

Detectors and classifiers: It is usual to attack classifiers, and all the attacks we are aware of attack on classifiers. However, for many applications, classifiers are not useful by themselves. Road sign is a good example. A road sign classifier would be applied to images that consist largely of a road sign (e.g. those of [29]). But there is little application need for a road sign classifier except as a component of a road sign detector, because it is unusual in practice to deal with images that consist largely of road sign. Instead, one usually deals with images that contain many things, and must find and label the road sign. It is natural to study road sign classifiers (e.g. [26]) because image classification remains difficult and academic studies of feature constructions are important. But there is no particular threat posed by an attack on a road sign classifier. An attack on a road sign detector is an entirely different matter. For example, imagine the danger if one could get a template that, with a can of spray paint, could ensure that a detector reads a stop sign as a yield sign (or worse!). As a result, it is important to know whether (a) such examples could exist and (b) how robust their adversarial property is in practice.

Recently, Evtimov *et al.* have shown several physical stop signs that are misclassified [6]. They cropped the stop signs from the frames before presenting them to the classifier. By cropping, they have proxied the box-prediction process in a detector; however, their attack is not intended as an attack on a detector (the paper does not use the word “detector”, for example). Lu *et al.* showed that their construction does not fool a standard detector [17], likely because the cropping process does not proxy a detector’s box selection well, and suggested that constructing an adversarial example that fools a detector might be hard. Figure 1 shows their stop signs presented in [6] are reliably detected by Faster RCNN.

3. Method

We propose a method to generate digital and physical adversarial examples that are robust to changes of viewing



Figure 1. Evtimov *et al.* [6] generated physical stop signs that are misclassified, however, these stop signs are reliably detected by Faster RCNN. Images from Figure 10 in [17].

conditions. Our registration and reconstruction based approach generates adversarial perturbations from video sequences of an object with moving cameras. We require the objects in the videos to be accurately aligned in 3D space. We can easily register stop signs as they are 2D polygons. Moreover, we can accurately register face images to a virtual 3D face model. Hence, we perform our experiments on these two types of data.

3.1. Approach for stop signs

We use the stop sign example to demonstrate our attack, which extends to other objects that are registered from image domain to some root coordinate system (e.g. faces in section 3.2). We search for an adversarial pattern that (a) looks like a stop sign and (b) fools Faster RCNN. We select a set of N diverse frames \mathcal{I} as the training examples to generate the pattern. A stop sign is represented as a texture map \mathcal{T} in some root coordinate system. We construct (currently by hand) correspondences between eight vertices on the stop sign instances in training frames and the vertices of \mathcal{T} . We use these correspondences to estimate a viewing map \mathcal{M}_i , which maps the texture \mathcal{T} in the root coordinate system to the appropriate pattern in training frame \mathcal{I}_i . We also incorporate in \mathcal{M}_i the illumination intensity, which is estimated by computing the average intensity over the stop sign in the image. Relative illumination intensities are used to scale the adversarial perturbations. We write $\mathcal{I}(\mathcal{M}_i, \mathcal{T})$ for the image frame obtained by superimposing \mathcal{T} on the frame \mathcal{I}_i using the mapping \mathcal{M}_i ; $\mathcal{B}_s(\mathcal{I})$ for the set of stop sign bounding boxes obtained by applying Faster RCNN to the image \mathcal{I} ; and $\phi_s(b)$ for the score produced by Faster RCNN’s classifier for a stop sign in box b . To produce an adversarial example, we minimize the mean score for a stop sign produced by Faster RCNN in all training images as a

function of \mathcal{T} , that is

$$\Phi(\mathcal{T}) = \frac{1}{N} \sum_{i=1}^N \text{mean}_{b \in \mathcal{B}_s(\mathcal{I}(\mathcal{M}_i, \mathcal{T}))} \phi_s(b)$$

possibly subject to some constraint on \mathcal{T} , such as being close to a normal stop sign in L_2 distance. We have also investigated minimizing the maximum score for all the stop sign proposals, and found that minimizing the mean score gives slightly better results.

Minimization procedure: First, we compute $\nabla_{\mathcal{T}}\Phi(\mathcal{T})$ by computing $\text{mean}_{b \in \mathcal{B}_s(\mathcal{I}(\mathcal{M}_i, \mathcal{T}))} \phi_s(b)$. The gradients in the frame coordinate system are mapped to the root coordinate system with inverse view mapping \mathcal{M}_i^{-1} , and then are cropped to the extent of \mathcal{T} in that coordinate system. We average gradients mapped from all N training frames. However, directly using the gradients to take large steps frequently stalls the optimization process. Instead, we find that computing the descent direction with the sign of the gradients for given pattern $\mathcal{T}^{(n)}$ (n stands for iteration number) facilitates the optimization process.

$$\mathbf{d}^{(n)} = \text{sign}(\nabla_{\mathcal{T}}\Phi(\mathcal{T}^{(n)})).$$

We choose a very small step length ϵ such that $\epsilon\mathbf{d}^{(n)}$ represents an update of one least significant bit, which leads to an optimization step of form

$$\mathcal{T}^{(n+1)} = \mathcal{T}^{(n)} + \epsilon\mathbf{d}^{(n)}.$$

The optimization process usually takes hundreds or even thousands of steps. One termination criterion is to stop the optimization when the pattern fools the detector more than 90% of the cases on the validation set. Another termination criterion is a fixed number of iterations.

Why large steps are hard: In our experiments, taking large steps with unsigned gradients stalls the optimization process, and we believe large steps are hard to take for two reasons. First, each instance of the pattern occurs at a different scale, meaning that there must be some up- or down-sampling of the gradients when mapped to the root coordinate system. Although we register the images with subpixel accuracy, and use a bilinear method to interpolate the transformation process, signal losses are still inevitable. In section 4.2, we show some evidence that this effect may make our patterns more, rather than less, robust. Second, the structure of the network means that the gradient is a poor guide to the behavior of $\phi_s(b)$ over large scales. In particular, a ReLU network divides its input space into a very large number of cells, and values at any layer before the softmax layer are a continuous piecewise linear function within a cell. Because the network is trained to have a (roughly) constant output for large pieces of its input space,

the gradient must wiggle from cell to cell, and so may be a poor guide to the long scale behavior of the function.

Constraining distance to the original stop sign: In order to create less perceivable adversarial perturbations, we constrain the distance to the original stop sign to be small. An L_2 distance loss is added to the cost function, and we minimize

$$\Phi(\mathcal{T}) + \lambda \|\mathcal{T} - \mathcal{T}^{(0)}\|^2$$

Our experiments show that this distance constraint still cannot help to create small perturbations, but greatly changes the pattern of the perturbations, refer to Figure 6.

We create our physical adversarial stop signs by printing the pattern \mathcal{T} , cutting out the printed stop sign area, and sticking it to an actual stop sign (30 in by 30 in).

3.2. Extending to faces

We extend the experiments onto faces, which have complex geometries and larger intra class variances, to demonstrate that our analysis generalizes to other classes. In the face setting, we search for a pattern that fools a Faster RCNN based face detector [12] and looks like the original face. Our root coordinate system for faces is a virtual high quality face mesh generated from morphable face model [2]. For video sequences of a face, we reconstruct the geometry of the face in the input frames using morphable face model built from the FaceWarehouse [3] data. The model produces a 3D face mesh $F(w_i, w_e)$ that is a function of identity parameters w_i , and expression parameters w_e . FaceTracker [25] is used to detect landmarks l_i on the face frames, then we recover parameters and poses of the face mesh by minimizing the distances between the projected landmark vertices and their corresponding landmark locations on the image planes. This construction gives us pixel-to-mesh and mesh-to-pixel dense correspondences between all face frames and the root face coordinate system (shared face mesh). By projecting image pixels to the face meshes via barycentric coordinates, we can achieve subpixel accurate pixel-to-pixel registrations between all face frames (via root coordinate system). This correspondences are used to transfer the gradients from face image coordinates to the root coordinate system, then we merge the gradients from multiple images and reverse transfer the merged gradients back to the face image coordinates.

4. Results

In this section, we describe in depth the experiments we did and the results we got. Our supplementary materials include videos and more results, and it can be downloaded from http://jiajunlu.com/docs/advDetector_supp.zip. Our high resolution paper can be downloaded from <http://jiajunlu.com/>

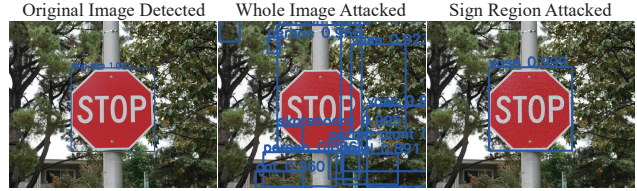


Figure 2. Modifying a single stop sign image to attack Faster RCNN is successful. In the original stop sign image (first), the stop sign is reliably detected. In the second image, small perturbations are added to the whole image, and the stop sign is not detected. In the last image, small perturbations are added to the stop sign region instead of the whole image, and the stop sign is detected as a vase.



Figure 3. Modifying a face image to attack Faster RCNN is successful. In the original face image (first), the face is reliably detected. In the second image, small perturbations are added to the whole image, and the face is not detected. In the last image, slightly larger perturbations are added to the face region instead of the whole image, and the face is not detected.

[docs/advDetector.pdf](#). But let us first give a quick overview of our findings:

- Adding small perturbations suffices to fool a given object detector on a single image.
- Enforcing the adversarial perturbations to generalize across view conditions requires significant changes to the pattern.
- Our successful attacks for Faster RCNN generalize to YOLO.
- Our successful attacks with very large perturbations generalize to the physical world objects in suitable circumstances.
- Simple defenses fail to defeat adversarial examples that can generalize.

Detectors are affected by internal thresholds. Faster RCNN uses a non maximum suppression threshold and a confidence threshold. For stop signs, we used the default configurations. For faces, we found the detector is too willing to detect faces, and we made it less responsive to faces (nms from 0.15 to 0.3, and conf from 0.6 to 0.8). We used default YOLO configurations.



Figure 4. Adversarial examples of stop signs for Faster RCNN that can generalize across view conditions. The original sequence in the first row is a test video sequence captured for a real stop sign, and the stop sign is detected in all the frames. We apply our attack to a training set of videos to generate a cross view condition adversarial perturbation, and apply that perturbation on this test sequence to generate the attacked sequence in the second row. This is a digital attack, and the stop sign is either not detected or detected as a kite.



Figure 5. Adversarial examples of faces for Faster RCNN based face detector [12] that can generalize across view conditions. The original sequence images in the first row are sampled from a test video sequence, and all the faces are reliably detected. We apply our attacking method to a training set of videos to generate a cross view condition adversarial perturbation, and apply that perturbation on this test sequence to generate the attacked sequence in the second row. This is a digital attack.

4.1. Attacking single image

We can easily adjust a pattern on a single image to fool a detector (stop signs in Figure 2 and faces in Figure 3), and the change on the pattern is tiny. While this is of no practical significance, it shows our search method can find very small adversarial perturbations.

4.2. Generalizing across view conditions

What we are really interested in is to produce a pattern that fails to be detected in any image. This is much harder because our pattern needs to generalize to different view conditions and so on. We can still find adversarial patterns in this situation, but the patterns found by our process involve significant changes of the stop signs and faces.

Stop sign dataset: we use a Panasonic HC-V700M HD camera to take 22 videos of the camera approaching stop signs, and extract 5 diverse frames from each video. Then we manually register all the stop signs, and use our attacking method to generate a unified adversarial perturbation for all the frames. We use 12 videos for generating adversarial perturbations (training), 5 videos for validation, and 5 videos for evaluation (testing). We use the validation set



Figure 6. We generate three adversarial stop signs with our attacking method. The first stop sign does not use L_2 distance penalty, and use termination criterion of successfully attacking 90% of validation images. The second stop sign uses L_2 distance penalty in the objective function, and terminates when 90% of validation images are attacked. The last stop sign also adopts L_2 distance penalty, but performs a large fixed number of iterations. All three patterns reliably fool detectors when mapped into videos. However, physical instances of these patterns are not equally successful. The first two stop signs, as physical objects, only occasionally fool Faster RCNN; the third one, which has a much more extreme pattern, is more effective.

termination criteria described in Section 3.1. Figure 4 gives an example video sequence, and its corresponding attacked video sequence. Table 1 shows the stop sign detection rates in different circumstances. We plan to release the labelled

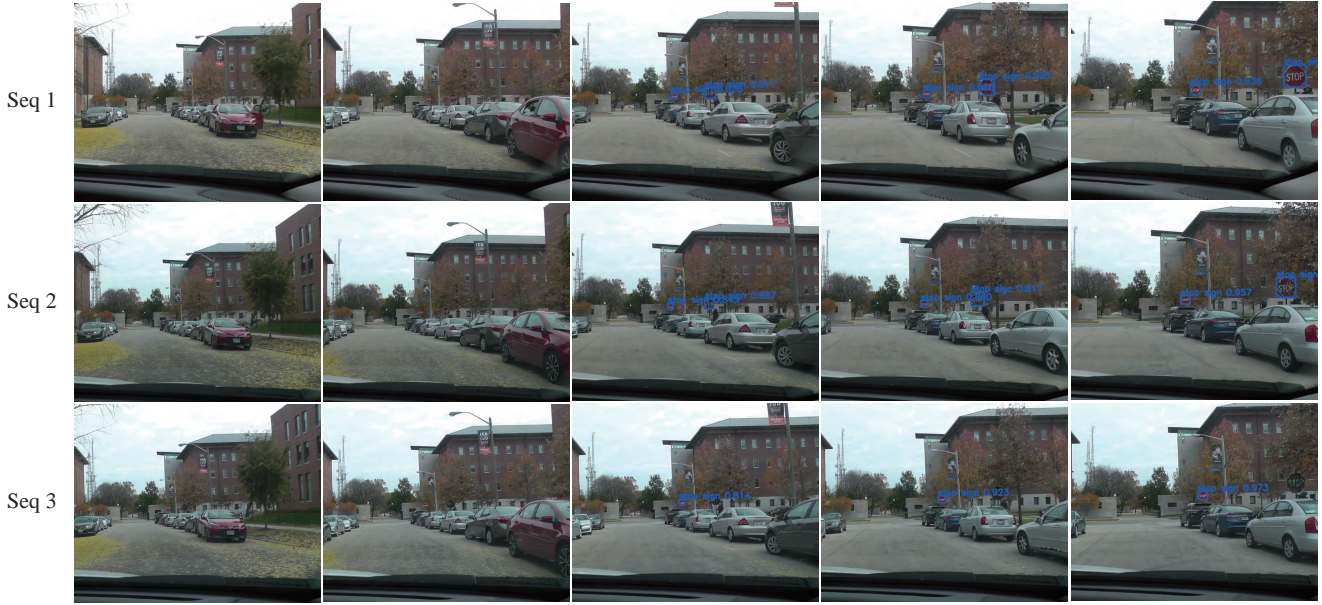


Figure 7. We print the three adversarial stop signs from Figure 6, and stick them to a real stop sign. We took videos while driving by these printed stop signs, and ran Faster RCNN on these videos. Notice that all of the adversarial perturbations generalize well digitally. We only render the detection results for stop signs to make the figures clean. The three sequences in this figure correspond to the three stop signs in order. In the first two sequences, stop signs are detected without trouble, while in the last sequence, the stop sign is not detected in the video, so it is a physical adversarial stop sign. This may be the result of poor texture contrast against the tree, though this sequence was not seen in training.

dataset.

Face dataset: we use a SONY a7 camera to take 5 videos of a still face from different distances and angles, and extract 20 diverse frames from each video. We use the morphable face model approach to register all the faces, and use our attacking method to generate a unified adversarial perturbation. We use 3 videos for generating adversarial perturbations (training), 1 video for validation, and 1 video for evaluation (testing). Again, we use the validation set termination criteria described in Section 3.1. Figure 5 shows an example video sequence, and its corresponding attacked video sequence. In our experiments, this is the smallest perturbations on faces that could generalize. Table 2 shows the face detection rates in different circumstances. Also, we plan to release the processed dataset.

In summary, it is possible to attack stop signs and faces from multiple images, and require them to generalize to new similar view condition images. However, both of them require strong perturbation patterns to generalize. Refer to supplementary materials for details.

4.3. Generalizing to the physical world

There is a big gap between attacks in the digital world and attacks in the physical world, which means the adversarial perturbations that generalize well in the digital world may not generalize to the physical world. We suspect this gap is due to various practical concerns, such as sensor

properties, view conditions, printing errors, lighting, etc. In this paper, we print stop signs and perform physical experiments with them, but we believe similar conclusions apply to faces.

We performed physical experiments with three adversarial perturbation patterns in Figure 6. Our results in Table 3 show that the two less perturbed stop signs can still be detected by Faster RCNN, while the one with large perturbations is hard to detect. The frames for physical experiments could be found in Figure 7. Refer to our supplementary materials for videos.

We performed analysis with the data from Table 1 and Table 3. L_1 regularized logistic regression is used to predict the success of our many different cases. The most important variable is detector (generalization from Faster RCNN to YOLO is not strong); then whether the adversarial example is physical or not (digital attacks are more effective than physical); then scale (it is hard to make a detector to miss a nearby stop sign).

4.4. Generalizing to YOLO

Adversarial examples for a certain classifier generalize across different classifiers. To test out whether adversarial examples for Faster RCNN generalize across detectors, we feed these images into YOLO. We categorize our adversarial examples into three categories: single image examples with small perturbations, multiple image examples

		test - far	test - medium	test - near	train - far	train - medium	train - near	val - far	val - medium	val - near
Tree bg - L	Stop1	0/4 ; 4/4	0/4 ; 1/4	0/2 ; 2/2	0/10 ; 6/10	0/10 ; 1/10	0/5 ; 5/5	1/4 ; 3/4	0/4 ; 3/4	0/2 ; 2/2
	Stop2	0/4 ; 4/4	1/4 ; 3/4	0/2 ; 2/2	2/10 ; 1/10	1/10 ; 0/10	2/5 ; 3/5	0/4 ; 1/4	0/4 ; 0/4	0/2 ; 0/2
Tree bg - EL	Stop3	n/a ; n/a	n/a ; n/a	n/a ; n/a	1/5 ; 5/5	0/5 ; 0/5	0/4 ; 1/4	n/a ; n/a	n/a ; n/a	n/a ; n/a
Sky bg - L	Stop1	0/6 ; 6/6	0/6 ; 5/6	0/3 ; 3/3	0/14 ; 13/14	0/14 ; 12/14	0/7 ; 6/7	0/6 ; 6/6	0/6 ; 5/6	0/3 ; 2/3
	Stop2	0/6 ; 6/6	0/6 ; 6/6	0/3 ; 3/3	0/14 ; 13/14	2/14 ; 12/14	1/7 ; 6/7	0/6 ; 6/6	0/6 ; 5/6	1/3 ; 2/3
Sky bg - EL	Stop3	0/4 ; 3/4	0/4 ; 1/4	0/4 ; 3/4	0/5 ; 5/5	0/5 ; 5/5	0/4 ; 4/4	n/a ; n/a	n/a ; n/a	n/a ; n/a

Table 1. This table reports the detection rates of Faster RCNN and YOLO for the multiple image digital attacks of stop signs. In each cell, the ratio before semicolon represents the detection rate for Faster RCNN, and the ratio after semicolon represents the detection rate for YOLO. Tree bg means the background of the stop sign is tree and has low contrast, and the Sky bg means the background of the stop sign is sky and has high contrast. L following the background means the perturbations are large, and EL means the perturbations are extremely large. We have three dark stop signs, and the detection rates are calculated at three different distances (far/medium/near) on train/val/test splits. We can attack Faster RCNN with multiple view conditions, and the adversarial perturbations generalize to new view conditions. The adversarial examples also generalize to YOLO, especially when the background is tree.

	test				train				val			
	ft-far	ft-near	sd-far	sd-near	ft-far	front-near	sd-far	sd-near	ft-far	ft-near	sd-far	sd-near
S100 small perturbation	2/3	2/4	6/6	6/7	0/19	0/21	0/9	0/11	1/4	6/8	3/4	3/4
S100 medium perturbation	3/3	2/4	6/6	3/7	5/19	1/21	1/9	0/11	2/4	4/8	4/4	3/4
S100 large perturbation	0/3	0/4	1/6	0/7	0/19	0/21	0/9	0/11	0/4	0/8	0/4	0/4
S15 large perturbation	0/1	n/a	0/2	n/a	0/3	0/2	0/2	0/2	0/1	n/a	0/2	n/a

Table 2. This table reports the detection rates of Faster RCNN based face detector [12] for multiple image digital attacks of faces. S100 means there are 100 images in the experiments, and S15 means there are 15 images. Ft means frontal face, and sd means side face. When small perturbations are applied, attacks on all the training images succeed, but do not generalize to the validation and testing images. Only when large perturbations are applied, the attacks generalize to different view conditions.

		far - adv	far - clean	medium - adv	medium - clean	near - adv	near - clean
Tree bg - L	Dark-Stop1	2/17 ; 4/17	16/17 ; n/a	11/12 ; 12/12	12/12 ; n/a	8/8 ; 8/8	8/8 ; n/a
	Dark-Stop2	4/17 ; 5/17	n/a ; n/a	6/11 ; 10/11	n/a ; n/a	0/14 ; 12/14	n/a ; n/a
	Bright-Stop1	10/17 ; 16/17	17/17 ; n/a	15/15 ; 15/15	15/15 ; n/a	12/12 ; 12/12	12/12 ; n/a
	Bright-Stop2	1/17 ; 2/17	14/17 ; n/a	10/12 ; 12/12	12/12 ; n/a	5/8 ; 8/8	8/8 ; n/a
Tree bg - EL	Dark-Stop3	0/17 ; 0/17	17/17 ; n/a	4/14 ; 10/14	14/14 ; n/a	8/11 ; 7/11	11/11 ; n/a
	Bright-Stop3	0/17 ; 0/17	11/17 ; n/a	1/11 ; 3/11	11/11 ; n/a	0/7 ; 1/7	7/7 ; n/a
Sky bg - L	Dark-Stop1	1/19 ; 5/19	0/19 ; n/a	9/11 ; 11/11	0/13 ; n/a	16/16 ; 16/16	14/16 ; n/a
	Dark-Stop2	0/25 ; 14/25	2/25 ; n/a	5/15 ; 11/15	1/15 ; n/a	24/24 ; 11/24	22/24 ; n/a
	Bright-Stop1	5/26 ; 23/26	0/26 ; n/a	10/11 ; 11/11	1/11 ; n/a	21/21 ; 21/21	14/21 ; n/a
	Bright-Stop2	1/23 ; 16/23	0/23 ; n/a	10/11 ; 9/11	0/11 ; n/a	20/24 ; 19/24	18/24 ; n/a
Sky bg - EL	Dark-Stop3	14/27 ; 16/27	20/27 ; n/a	3/13 ; 11/13	13/13 ; n/a	26/27 ; 26/27	27/27 ; n/a
	Bright-Stop3	0/28 ; 11/28	0/24 ; n/a	0/13 ; 10/13	2/13 ; n/a	22/24 ; 10/24	18/24 ; n/a

Table 3. The detection rates of the physical adversarial stop signs and physical clean stop signs with Faster RCNN and YOLO in different circumstances. The table layout is similar to Table 1. We have two stop signs with different brightness for large perturbations, and one stop sign with different brightness for extremely large perturbations. We report both detection rates for 30 x 30 inches adversarial stop signs (adv) and 20 x 20 inches clean normal stop signs when applicable (clean).

with large perturbations that generalize across viewing conditions digitally, and physical examples with large perturbations. Our experiments show that small perturbations do not generalize to YOLO, while obvious perturbation patterns can generalize to YOLO with good probability. Examples are given in Figure 8, and detection rates can be found in Table 3 and Table 1.

4.5. Localized attacks fail

In previous settings, we attack the whole masked objects in the images, however, it is usually hard to apply such attacks in the physical world. For example, modifying the whole stop sign patterns is useless in practice, and wearing a whole face mask with perturbation patterns is hard too. It would be more effective attack if one can manufacture small stickers with perturbation patterns, and when the sticker is attached to a small region of the stop sign or the face fore-



Figure 8. We test whether adversarial examples generated from Faster RCNN generalize to YOLO. In the first row, these adversarial examples are generated for a single image with small perturbations. YOLO can detect these stop signs without trouble. In the second row, these adversarial examples are generated from multiple images, and the digitally perturbed images can fool YOLO in about half of the times. In the last row, physically printed adversarial stop signs can still fool YOLO in some circumstances. The detailed summary can be found in Table 1 and Table 3.



Figure 9. Localized attacks for stop signs and faces fail in the multiple view condition setting. We applied attacks on regions of the stop signs and faces with very large number of iterations, and introduced extremely large perturbations, but the objects are still detected. In detail, localized attacks on stop signs can sometimes digitally fool far stop signs, but not for middle and near stop signs; localized attacks on faces cannot fool face detector. The first image is an example of perturbed stop signs, and the second image is an example of perturbed faces.

head, the detector would fail. Evtimov *et al.* [6] showed an example that successfully attacked stop sign classifiers. We try to generate adversarial patterns constrained to a fixed region of the objects to fool detectors, however, we find these attacks only occasionally successful (stop signs) or wholly unsuccessful (faces). Figure 9 shows some examples.

4.6. Simple defenses fail

Recently, Guo *et al.* [11] showed that simple image processing could defeat a majority of imperceivable adversarial attacks. We assume detectors should run at frame rate, so exclude image quilting. We investigated down-up sampling and total variation smoothing defense. We find that these methods can defeat attacks on a single image, but cannot

		NonAttack	Adversarial	UP	TV
Single		10/10	0/10	10/10	10/10
Multiple	stop1	110/110	1/110	8/110	8/110
	stop2	110/110	10/110	18/110	9/110
	stop3	40/40	1/40	1/40	2/40
Physical	stop1	109/187	121/185	118/185	116/185
	stop2	77/159	86/201	84/201	88/201
	stop3	151/205	78/209	72/209	85/209

Table 4. We evaluate the effectiveness of simple defense methods. UP means downsample the input image resolution by half, and then upsample it to the original size. TV means total variation denoise, which removes high frequency information. The physical non attack numbers are counted from a real stop sign near our adversarial one. These simple defense methods are effective for single image perturbations, but not effective for multiple image perturbations that can generalize. They also cannot defeat physical adversarial perturbations.

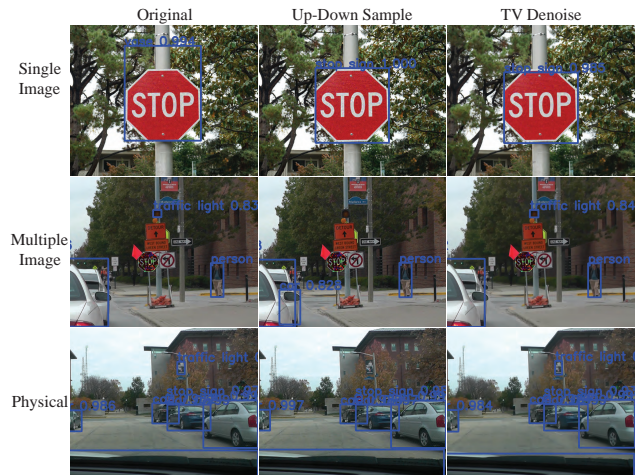


Figure 10. We apply simple defenses [11] to adversarial examples generated for Faster RCNN. Up-Down Sample means down sample the image resolution by half, and then upsample it to the original resolution. TV Denoise means denoising the image with total variation regularization, which will remove the high frequency information and keep the low frequency information. In the first row, the adversarial examples generated from a single image with small perturbations can be detected after simple image processing. In the second row, the adversarial examples generated from multiple view conditions still cannot be detected after simple defense. In the last row, the physically printed adversarial stop signs still cannot be detected after simple defense.

disrupt the large patterns needed to produce adversarial examples that generalize, see Figure 10 and Table 4. Our hypothesis for this phenomenon is that tiny perturbations work with numerical accumulation mechanism, which is not robust to changes, while obvious perturbations work with pattern recognition mechanism, which is more robust and can better generalize.

5. Conclusion

We have demonstrated the first adversarial examples that can fool detectors. Our construction yields physical objects that fool detectors too. However, all the adversarial perturbations we have been able to construct require large perturbations. This suggests that the box prediction step in a detector acts as a form of natural defense. We speculate that better viewing models in our construction may yield a smaller gap between physical and digital results. Our patterns may reveal something about what is important to a detector.

References

- [1] A. Athalye and I. Sutskever. Synthesizing robust adversarial examples. *arXiv preprint arXiv:1707.07397*, 2017. 1, 2
- [2] V. Blanz and T. Vetter. A morphable model for the synthesis of 3D faces. In *SIGGRAPH*, pages 187–194. ACM, 1999. 4
- [3] C. Cao, Y. Weng, S. Zhou, Y. Tong, and K. Zhou. Facewarehouse: A 3d facial expression database for visual computing. *IEEE Transactions on Visualization and Computer Graphics*, 20(3):413–425, Mar. 2014. 4
- [4] N. Carlini and D. Wagner. Defensive distillation is not robust to adversarial examples. 2
- [5] X. Chen and A. Gupta. An implementation of faster rnn with study for region sampling. *arXiv preprint arXiv:1702.02138*, 2017. 1
- [6] I. Evtimov, K. Eykholt, E. Fernandes, T. Kohno, B. Li, A. Prakash, A. Rahmati, and D. Song. Robust physical-world attacks on machine learning models. *arXiv preprint arXiv:1707.08945*, 2017. 2, 3, 8
- [7] A. Fawzi, O. Fawzi, and P. Frossard. Analysis of classifiers’ robustness to adversarial perturbations. *arXiv preprint arXiv:1502.02590*, 2015. 2
- [8] A. Fawzi, S. Moosavi-Dezfooli, and P. Frossard. Robustness of classifiers: from adversarial to random noise. *CoRR*, abs/1608.08967, 2016. 2
- [9] I. J. Goodfellow, J. Shlens, and C. Szegedy. Explaining and harnessing adversarial examples. *arXiv preprint arXiv:1412.6572*, 2014. 2
- [10] S. Gu and L. Rigazio. Towards deep neural network architectures robust to adversarial examples. *CoRR*, abs/1412.5068, 2014. 2
- [11] C. Guo, M. Rana, M. Cisse, and L. van der Maaten. Countering adversarial images using input transformations. *arXiv preprint arXiv:1711.00117*, 2017. 2, 8
- [12] H. Jiang and E. Learned-Miller. Face detection with the faster r-cnn. In *Automatic Face & Gesture Recognition (FG 2017)*, 2017 12th IEEE International Conference on, pages 650–657. IEEE, 2017. 4, 5, 7
- [13] A. Kurakin, I. J. Goodfellow, and S. Bengio. Adversarial examples in the physical world. *CoRR*, abs/1607.02533, 2016. 2
- [14] Y. Liu, X. Chen, C. Liu, and D. Song. Delving into transferable adversarial examples and black-box attacks. *arXiv preprint arXiv:1611.02770*, 2016. 1
- [15] J. Lu, T. Issaranon, and D. Forsyth. Safetynet: Detecting and rejecting adversarial examples robustly. *arXiv preprint arXiv:1704.00103*, 2017. 2
- [16] J. Lu, H. Sibai, E. Fabry, and D. Forsyth. No need to worry about adversarial examples in object detection in autonomous vehicles. *arXiv preprint arXiv:1707.03501*, 2017. 2
- [17] J. Lu, H. Sibai, E. Fabry, and D. Forsyth. Standard detectors aren’t (currently) fooled by physical adversarial stop signs. *arXiv preprint arXiv:1710.03337*, 2017. 2, 3
- [18] J. H. Metzen, T. Genewein, V. Fischer, and B. Bischoff. On detecting adversarial perturbations. *arXiv preprint arXiv:1702.04267*, 2017. 2
- [19] S. Moosavi-Dezfooli, A. Fawzi, and P. Frossard. Deepfool: a simple and accurate method to fool deep neural networks. *CoRR*, abs/1511.04599, 2015. 1, 2
- [20] S.-M. Moosavi-Dezfooli, A. Fawzi, O. Fawzi, and P. Frossard. Universal adversarial perturbations. *arXiv preprint arXiv:1610.08401*, 2016. 1, 2
- [21] A. Nguyen, J. Yosinski, and J. Clune. Deep neural networks are easily fooled: High confidence predictions for unrecognizable images. In *CVPR*, 2015. 1, 2
- [22] N. Papernot, P. D. McDaniel, and I. J. Goodfellow. Transferability in machine learning: from phenomena to black-box attacks using adversarial samples. *arXiv preprint arXiv:1605.07277*, 2016. 1
- [23] J. Redmon and A. Farhadi. Yolo9000: better, faster, stronger. *arXiv preprint arXiv:1612.08242*, 2016. 1
- [24] S. Ren, K. He, R. Girshick, and J. Sun. Faster r-cnn: Towards real-time object detection with region proposal networks. In *Advances in neural information processing systems*, pages 91–99, 2015. 1
- [25] J. Saragih and K. McDonald. Facetracker. <https://github.com/kylemcdonald/FaceTracker>. 4
- [26] P. Sermanet and Y. LeCun. Traffic sign recognition with multi-scale convolutional networks. In *Neural Networks (IJCNN), The 2011 International Joint Conference on*, pages 2809–2813. IEEE, 2011. 2
- [27] U. Shaham, Y. Yamada, and S. Negahban. Understanding adversarial training: Increasing local stability of neural nets through robust optimization. *arXiv preprint arXiv:1511.05432*, 2015. 2
- [28] M. Sharif, S. Bhagavatula, L. Bauer, and M. K. Reiter. Accessorize to a crime: Real and stealthy attacks on state-of-the-art face recognition. In *Proceedings of the 2016 ACM SIGSAC Conference on Computer and Communications Security*, CCS ’16, pages 1528–1540, New York, NY, USA, 2016. ACM. 2
- [29] J. Stallkamp, M. Schlipsing, J. Salmen, and C. Igel. Man vs. computer: Benchmarking machine learning algorithms for traffic sign recognition. *Neural networks*, 32:323–332, 2012. 2
- [30] C. Szegedy, W. Zaremba, I. Sutskever, J. Bruna, D. Erhan, I. Goodfellow, and R. Fergus. Intriguing properties of neural networks. *arXiv preprint arXiv:1312.6199*, 2013. 2